Lab on a Chip

Check for updates

A surface-engineered contact lens for tear fluid biomolecule sensing†

Aravind M [iD][a] and Sajan D. George [iD] *[ab]

The eyes provide rich physiological information and offer diagnostic potential as a sensing site, and probing tear constituents *via* the wearable contact lens could be explored for healthcare monitoring. Herein, we propose a novel adhesive contrast contact lens platform that can split tear film by natural means of tear secretion and blinking. The adhesive contrast is realized by selective grafting of a lubricant onto a polydimethylsiloxane (PDMS)-based contact lens, leading to high pinning zones on a non-adhesive background. The difference in contact angle hysteresis facilitates the liquid splitting. Further, the method offers control over the droplet volume by controlling the zone dimension. The adhesive contrast contact lens is coupled with fluorescent spectroscopic as well as colorimetric techniques to realize its potential as a diagnostic platform. The adhesive contrast contact lens is exploited to detect the level of lactoferrin in tear by sensitizing split droplets with Tb^{3+} ions. The adhesive contrast contact lens integrated with a fluorescence spectrometer was able to detect the lactoferrin level up to a concentration of 0.25 mg mL^{-1}. Additionally, a colorimetric detection based on the fluorescence of the lactoferrin–terbium complex is demonstrated for the measurement of lactoferrin, with a limit of detection in the physiological range up to 0.5 mg mL^{-1}.

Introduction

The eye contains abundant physiological information and metabolite biomarkers that are currently being investigated *via* a wearable diagnostic platform such as a contact lens. Owing to the advances in electronics, microfabrication techniques, materials, and sensing technologies, the potential of contact lenses as a disease diagnostic platform *via* probing various biochemical/physical parameters has recently been under intense investigation.[1–3] Moreover, the tear fluid-contact lens interaction has been extensively studied for the development of self-moisturizing contact lenses, contact lens-based sensing platforms, lower protein adsorption, and antibacterial contact lenses.[4–11] The surface wettability of the contact lens plays a crucial role in the lens surface-tear film interaction.[12] Inspired by naturally occurring surfaces, researchers are employing various strategies to fabricate superhydrophobic, superhydrophilic, and wettability contrast surfaces.[13,14] The precise control of hydrophobic and hydrophilic properties at the interface through modification of the surfaces *via* chemical or physical methods has opened a myriad of applications, including water harvesting, microfluidic platforms, and concentration enrichment of analyte molecules for chemical analysis.[15–17] Among these, wettability contrast droplet assay platforms *via* selective modification of the surface *via* chemical or physical approaches and by utilizing the wettability or adhesion difference for droplet splitting have been gaining more attention recently. Such platforms offer unique advantages such as consuming less sample volume, facilitating parallel processing, generating more and better-quality data for comparative as well as multiplexed analysis, and having limited space requirements. The spontaneous splitting of a droplet into multiple smaller droplets and integration with various sensing platforms has shown great potential, especially when integrated with optical spectroscopic studies.[16,18] However, most of these studies were carried out on flat surfaces and thus limit real-life applications where the surfaces are non-flat. To the best of our knowledge, no studies have been reported on curved surfaces such as contact lenses that utilized them for tear fluid splitting *via* adhesion differences of the substrate or employed optical sensing for tear fluid constituent measurements.

In the burgeoning research field of wearable devices for healthcare monitoring and diagnosis, contact lenses are emerging as a preferred candidate. Contact lenses offer a sensing platform for intraocular pressure, temperature,

[a] Department of Atomic and Molecular Physics, Manipal Academy of Higher Education, Manipal, India – 576104. E-mail: sajan.george@manipal.edu
[b] Centre for Applied Nanosciences (CAN), Manipal Academy of Higher Education, Manipal, India – 576104

† Electronic supplementary information (ESI) available. See DOI: https://doi.org/10.1039/d4lc00176a

glucose, pH, and nitrites.[3] However, most of the sensing contact lens-based platform relies on the complex fabrication of microchannel networks for guiding tears to sensing chambers or multilayer material fabrication, as well as inorganic or 2D nanomaterials for sensing, whose toxic effects have not been investigated in detail.[19,20] In contrast, herein, a novel, simple and facile adhesive contrast contact lens concept is employed wherein the adhesive contrast facilitates the tear film splitting, and these zones act as platforms for spectroscopic analysis of the tear constituents. More importantly, the adhesive contrast is realized by chemically grafting biocompatible silicone oil selectively onto PDMS-based contact lenses *via* an oxygen plasma treatment approach. The lubricant grafting turns the PDMS surface non-adhesive and reduces the contact angle hysteresis, which, in turn, is expected to favour eyelid movement due to reduced friction. Conversely, the pristine or non-oil-grafted PDMS region remains a droplet-pinning region due to its inherent high contact angle hysteresis. The contact angle hysteresis difference between the lubricant-grafted background and pristine PDMS zones results in the splitting of the tear film. This novel approach allows the tears to be collected in the specified zones of the contact lens by completely natural means, such as normal secretion and blinking. The current work stands out from all published works because of its novel fabrication method, which allows the creation of adhesive contrast on curved surfaces as well as flat surfaces. Moreover, the adhesive contrast on the contact lens surface is a unique platform for tear fluid analysis. The study also reports that by integrating fluorescence spectroscopy with the adhesive contrast contact lenses, sensitive detection of lactoferrin can be achieved. Lactoferrin is a critical glycoprotein and a potential biomarker in ocular health screening, such as dry eye disease. Fluorescence spectroscopy coupled with the adhesive contrast contact lenses allows the detection of lactoferrin up to a concentration as small as 0.25 mg mL^{-1}. Additionally, a less sophisticated method of colorimetric detection of lactoferrin on the adhesive contrast contact lens is demonstrated with a lab-built, cost-effective illumination setup. It is envisaged that with further development, adhesive contrast contact lenses will facilitate a novel, cost-effective and reliable screening tool for advanced eye-care applications.

Experimental

Materials

Polydimethylsiloxane (PDMS, Sylgard 184, Dow Corning), silicone oil (350 cSt, Sigma Aldrich), human lactoferrin (Sigma Aldrich), terbium(III) chloride hexahydrate (TbCl$_3$·6H$_2$O, Sigma Aldrich), tris(hydroxymethyl)aminomethane buffer (TRIS, Sigma Aldrich), artificial tears (carboxy-methylcellulose sodium eye drops IP 0.5% w/v, Refresh Tears, Allergen), and acridine orange (Himedia).

Preparation of adhesive contrast contact lens

The fabrication of adhesive contrast PDMS contact lenses involves two steps: first, the fabrication of PDMS-based contact lenses, followed by the selective grafting of
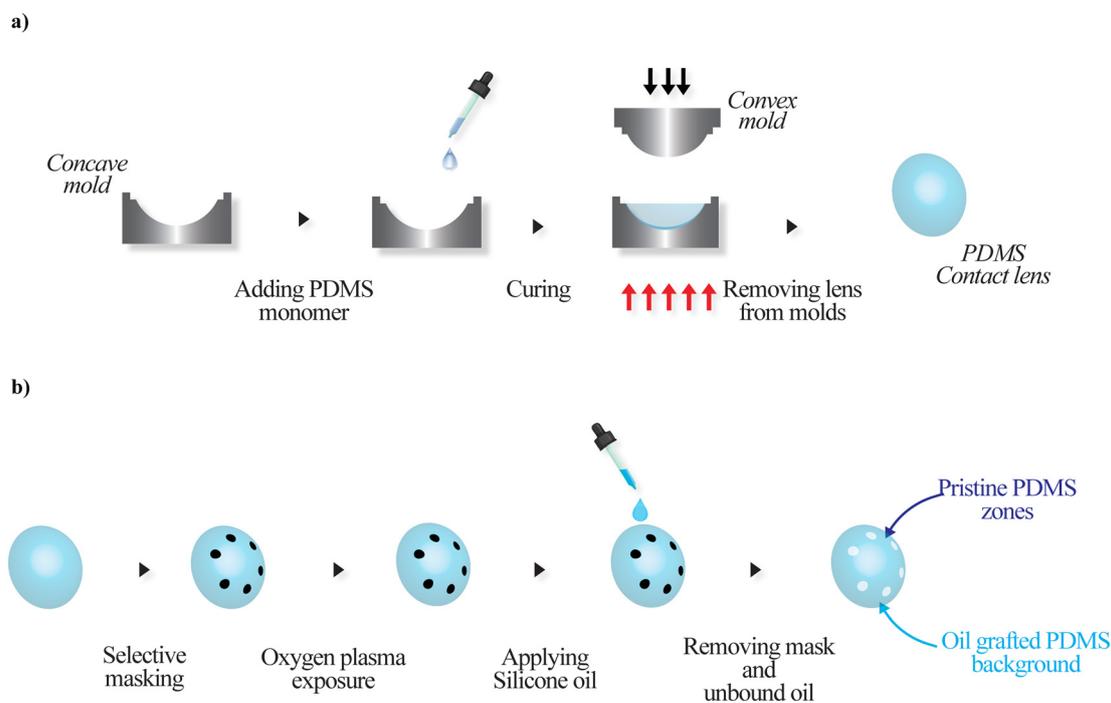

Fig. 1 Schematic of fabrication of a) a PDMS contact lens *via* mold casting and b) an adhesive contrast contact lens *via* selective lubricant grafting.

silicone oil (Fig. 1). The choice of PDMS for the present study stems from the fact that this material is transparent, flexible, biocompatible and has been used in a wide range of bio-applications. It has high oxygen permeability, making it advantageous for making contact lenses. PDMS has been extensively used in the literature for the fabrication of contact lenses, especially smart contact lenses, with applications in drug delivery and sensing.[21–25] Herein, the PDMS contact lenses were fabricated *via* the mold casting method using a pair of smooth convex and concave metallic molds, as shown in Fig. 1a. The molds were created with metallic parts using a lathe, followed by manual polishing. The molds were machined to deliver a contact lens with a cord diameter of 15 mm and a base radius of 8.5 mm. The separation between convex and concave molds determines the thickness of the contact lens, which, in this case, is ~70 μm. The PDMS base and a crosslinking curing agent were thoroughly mixed in a ratio of 10:1 and desiccated to

remove air bubbles. A few drops of the mixture were added to the concave mold, and the convex mold was pressed against the PDMS film. PDMS was cured at 80 °C for 30 min. After cooling to room temperature spontaneously, the PDMS contact lenses were carefully peeled off from the molds. The second step involves the selective grafting of silicone oil onto the contact lens surfaces; this circular spot of different diameters was made on the contact lens surface with a marker pen. The spots of different sizes ranging from 1 mm to 2.5 mm were placed outside the central optic zone (diameter 8 mm), as shown in Fig. 1b, so that the droplets after tear film splitting were not in the line of sight (optical zone) and did not impact the user's vision. The masked contact lenses were then exposed to oxygen plasma with a power of 90 W for 60 seconds (Femto low-pressure plasma system, Diener Electronic, Germany); immediately after this, a drop of silicone oil was spread on the lens surface and allowed to react for 24 hours under room conditions.
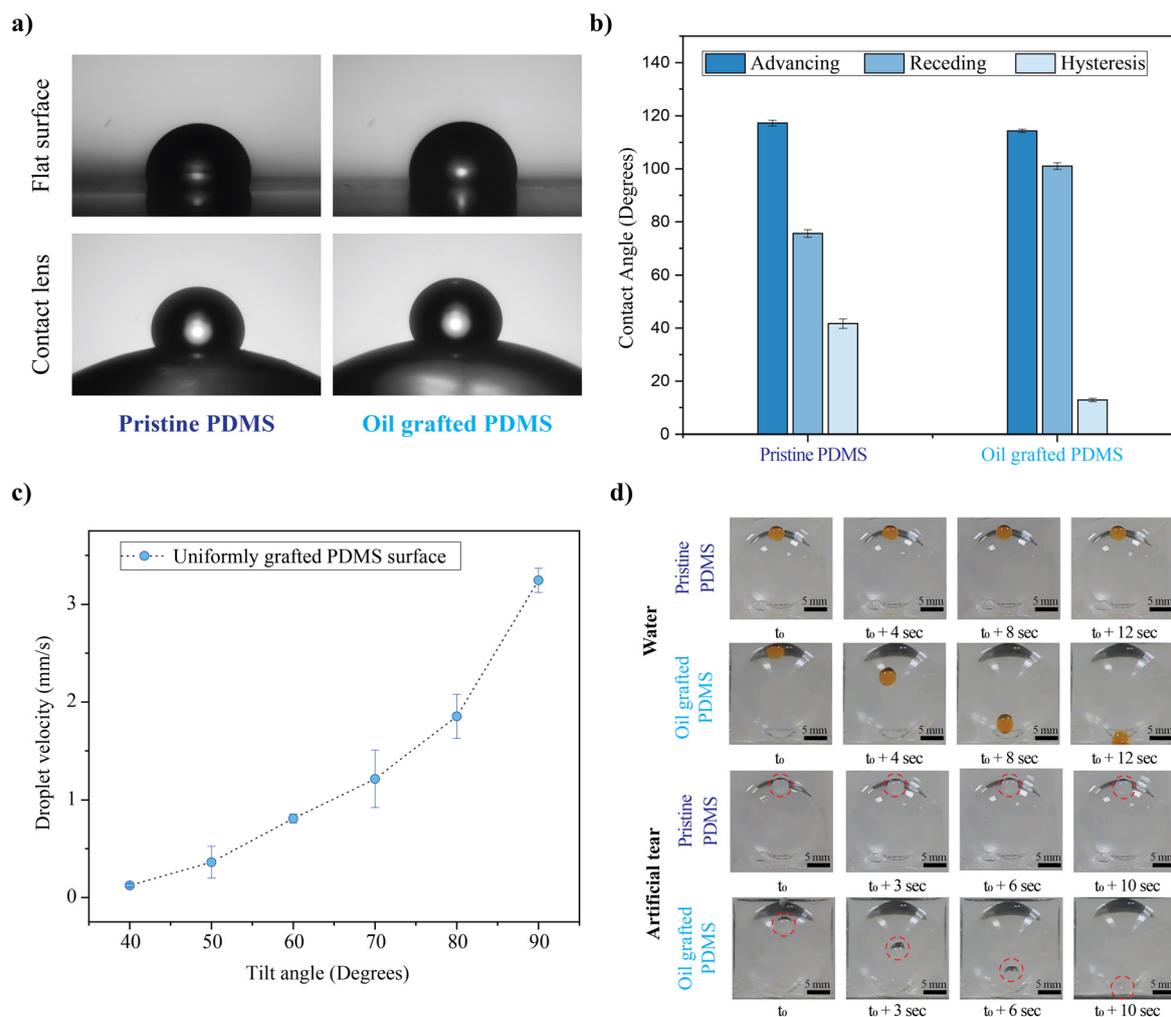

Fig. 2 a) Sessile drop images on pristine PDMS and oil-grafted PDMS on a flat surface and contact lens; b) advancing, receding, and contact angle hysteresis on a pristine as well as an oil-grafted PDMS surface; c) change in velocity of a 10 μL-water droplet with a tilt angle on a uniformly oil-grafted PDMS surface; and d) droplet pinning and non-adhesive behaviour of pristine and oil-grafted PDMS, respectively, towards water and artificial tear on a contact lens surface.

The unbound oil and mask were cleaned with toluene and Milli-Q water by ultrasonication.

Contact angle measurements

The nature of surface wetting was investigated using a commercial contact angle instrument (Holmarc, India). Static contact angles were determined with a 5 μL drop volume. The data were collected from at least three different positions on each sample. Advancing and receding contact angles were determined by increasing and decreasing the drop volume between 2 and 15 μL at a rate of 1 μL min^{-1}.

Results and discussion

The surface wettability of the silicone oil-grafted substrate was measured in terms of the equilibrium water contact angle (WCA), a 10 μL droplet onto the non-grafted and grafted substrate, which was found to be 108 ± 2° and 113 ± 2°, respectively (Fig. 2a). The WCA of the droplet was measured at different locations of the substrates, and there was no significant difference in terms of the WCA. The WCA values are well within the error bar. The contact angle hysteresis measurement reveals that even though there are no significant changes in terms of the WCA, advancing and receding contact angles changed after lubricant grafting (Fig. 2b). The large difference between advancing and receding contact angles on pristine PDMS yields a contact angle hysteresis of 41° (Fig. S1†). Conversely, lubricant grafting substantially changes the advancing and receding contact angles, especially an increase in the receding contact angle, resulting in a lower contact angle hysteresis of 12° (Fig. S2†). The change in the contact angle hysteresis confirms oil grafting, similar to our previous report.[15] To investigate the non-adhesive nature of the silicone oil-grafted substrate against a water droplet, the behaviour of a 10 μL water droplet was investigated for different tilt angles. It is observed that the water droplet starts to move downwards for a tilt angle of 40°, beyond which the droplet starts to slide spontaneously at a velocity that is found to increase exponentially with the sliding angle (Fig. 2c). The droplet velocity increases from 0.12 mm s^{-1} to 3.2 mm s^{-1} while changing the angle from 40° to 90°. It is pertinent to note here that the water droplet adheres strongly to the non-grafted substrate, and a 10 μL water droplet adheres to the substrate even when the substrate is tilted upside down (a tilt angle of 180°, Fig. S3†). To investigate the non-adhesive behavior on the contact lens surface, PDMS-based contact lenses were fabricated with a base radius of 8.5 mm and a cord diameter of 15 mm using the mold casting method, onto which the lubricant was grafted uniformly. The contact lenses uniformly grafted with lubricant exhibit sliding off of the droplet of water with an average velocity of nearly 1.5 mm s^{-1}, as shown in Fig. 2d (Video V1†). In contrast to the lubricant-grafted surface, the high contact angle hysteresis of pristine PDMS causes the pinning of the droplet on a curved contact lens surface. Fig. 2d also shows the non-adhesive
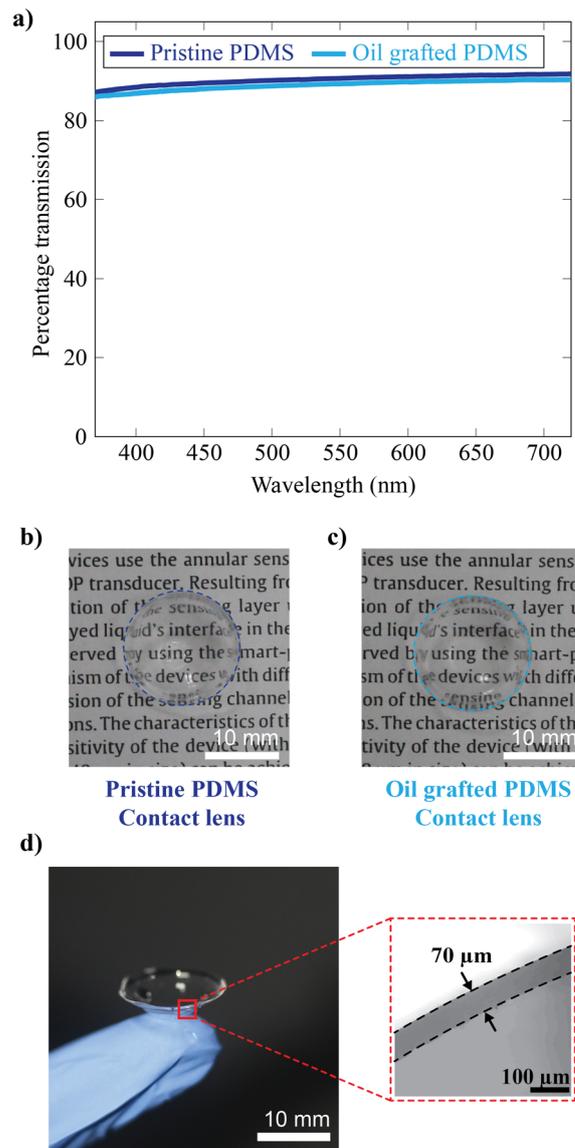

Fig. 3 a) Transmission spectra of pristine PDMS and oil-grafted PDMS; photographs of b) pristine and c) oil-grafted contact lenses; d) photograph of the fabricated contact lens, and a microscopic view of the cross-section of the contact lens.

property of uniformly grafted lenses against a drop of artificial tear solution, showing similar behavior to that of water (Video V1†).

Optical transparency is of crucial importance in the case of contact lenses, especially in the visible region. PDMS is intrinsically highly transparent in the visible region, and even after lubricant grafting, the transparency is not reduced, as evident from the transmission spectra (Fig. 3a). The grafted and pristine PDMS show good optical transparency, with a percentage transmission of ∼90%. The photographs of the lenses are also shown in Fig. 3b and c. Herein, the well-known compression moulding technique is adopted for contact lens fabrication. This technique allows the fabrication of thin contact lenses, where the thickness is
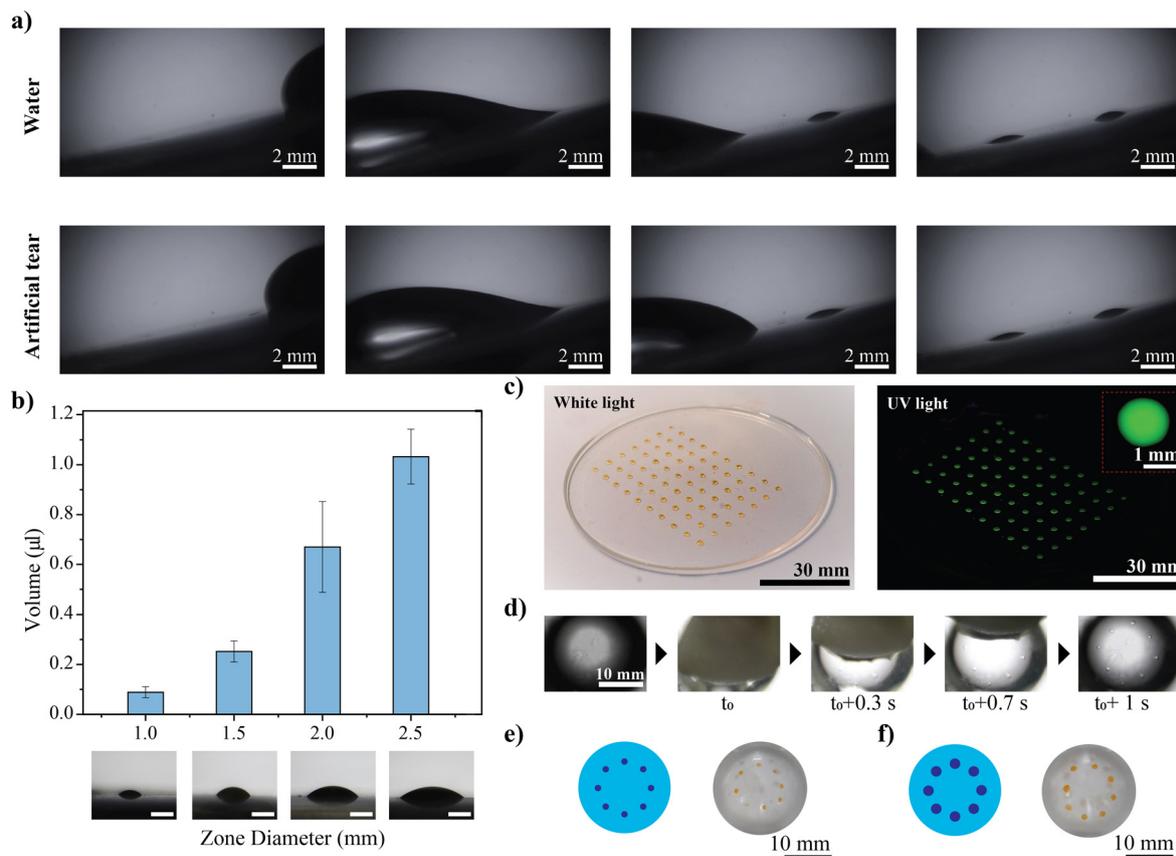
Fig. 4 a) A droplet of water and an artificial tear splitting to a smaller droplet while sliding across adhesive contrast surface of zone diameter 2 mm; b) variation in the volume of droplet after splitting with zone dimension (scale bar = 1 mm); c), droplet array on fabricated adhesive contrast surface after splitting a drop of fluorophore (acridine orange) photographed under visible and UV illumination (inset photograph of a single zone of diameter 1.5 mm); d) liquid film splitting on adhesive contrast contact lens and photograph of the adhesive contrast contact lens with zone dimensions of e) 1 and f) 2 mm after splitting water mixed with food coloring.

determined by the spacing between the convex and concave molds. The central thickness of fabricated lenses is ~70 microns (Fig. 3d).

The droplet splitting on the selective oil-grafted surface arises from the contrast in the adhesion force between the oil-grafted and pristine regions during the sliding of the master droplet. F_{CAH}, the contact angle hysteresis force, is measured in terms of advancing (θ_a) and receding (θ_r) angles using the expression $F_{CAH} = \gamma d(\cos\theta_r - \cos\theta_a)$, where γ (72.8 mN m^{-1}) and d (2.94 mm for 10 μL) are the surface tension of the liquid and contact line width, respectively.[15] Herein, the hysteresis force for a 10 μL water droplet on the oil-grafted substrate is estimated to be 4.7 μN, whereas the estimated hysteresis force for the pristine surface is found to be 16.4 μN. The oil grafting reduces the contact angle hysteresis force by nearly 3.5 times. Therefore, the sliding droplet onto the selectively oil-grafted surface becomes pinned at pristine zones with high contact angle hysteresis. The pinned droplet film eventually breaks to form droplets in each zone, and the volume and size of the droplet depend upon the dimension of the zone. When a larger water droplet slides across the surface, no residue is left behind in the oil-

grafted region after the droplet moves away, and the split droplets adhere completely to the pristine PDMS region. The artificial tear also shows similar behaviour (Fig. 4a, Video V2†). The corresponding volume of the droplet in each zone is found to vary with the dimension of the zone. The results of the study with different dimensions of the zones are shown in Fig. 4b. Since the zones are designed as circles, the split droplets are similar to a spherical cap in shape, with a base radius equivalent to the zone radius; hence, the volume of the split droplets is calculated by the equation, $V = \frac{\pi h}{6}(3a^2 + h^2)$, where h and a are the height and base radius of the droplets, respectively. The droplet volume is found to increase from 0.08 ± 0.02 μL to 1 ± 0.1 μL as we change the zone diameter from 1 to 2.5 mm (Fig. S4†). Fabricating multiple zones on a single substrate can add up to a droplet array platform, leading to an arrangement of multiple droplets of the desired volume to develop future analytic platforms. By exploiting the contrast in the surface, a droplet array platform is fabricated, wherein a larger droplet can split into multiple smaller droplets and can reside in predefined positions. Herein, a fluorescent dye (acridine orange) split across the platform

demonstrates the potential of these surfaces as a fluorescence spectroscopic assay platform, as shown in Fig. 4c. Further, selective grafting of oil on the PDMS contact lens led to the fabrication of a droplet array onto a cured surface similar to a contact lens. To mimic the eyelid movement, wet cotton is quickly spread across the contact lens surface, resulting in the film splitting and sticking of daughter droplets only to the pristine zones while leaving no residues observed on the oil-grafted region (Fig. 4d). Contact lenses with various zone diameters (1 mm and 2 mm) are fabricated here, and the zones are always designed to position outside the optical zone (diameter 8 mm) so as not to interfere with the user's visual experience (Fig. 4e). To further mimic eyelid movements, a set of studies was conducted. Two experiments were performed to achieve this. The first experiment evaluated the performance of the adhesive contrast contact lens at different blinking speeds, ranging from 15 mm s^{-1} to 230 mm s^{-1}, to account for the average speed of the opening and closing phases of blinking.[26] A contact lens with a non-grafted zone is fabricated and further immersed and taken out of a water bath at different speeds by mounting the lens onto a motorized stage. The volume of droplets split on the non-grafted zone is measured for different trials for a range of speeds comparable to the blinking speed (Fig. S5†). The second experiment investigated the stability and performance of the adhesive contrast substrate against constant and continuous blinking, for which the substrate was subjected to 15 000 blinking cycles. Herein, the adhesive contrast surface is immersed and taken out of the water bath, where the

substrate's wetting and dewetting mimic the closing and opening phases of blinking, respectively. The substrates were mounted on a motorised stage and moved in and out of the water bath at a speed of ~80 mm s^{-1}. The volume split on the non-grafted zone was measured at different cycles, during which the volume remained constant (Fig. S6†). Both studies ensured the consistent performance and stability of the adhesive contrast contact lens.

To explore the potential of the adhesive contrast contact lens as a diagnostic platform, the contact lens is coupled with a spectrofluorometer to detect the lactoferrin level in the tear. Lactoferrin is one of the most studied proteins because of its antioxidant, antibacterial, and anti-inflammatory properties.[27,28] The level of lactoferrin is between 1.01 and 2.15 mg mL^{-1} in healthy adults aged from 20 to 28 years old, with a decreasing rate of 0.01 mg mL^{-1} annually after the age of 29 years.[28–30] Moreover, changes in the level of lactoferrin are reported to be related to conditions such as dry eye disease.[31–33] The detection mechanism employed here relies on the enhanced fluorescence emission from complexes formed between lactoferrin deposited on sensing zones of the lens and trivalent terbium (Fig. S7†). The concentration-dependent emission of lactoferrin and Tb^{3+} complex allows rapid detection of lactoferrin levels in tears and is reported to have been adopted in fabricating microfluidic paper devices.[34,35] The detection procedure is depicted in Fig. 5a, wherein wearing the contact lens allows the collection of tears on the predefined zones *via* secretion and blinking. Once the zones collect the tear containing lactoferrin,
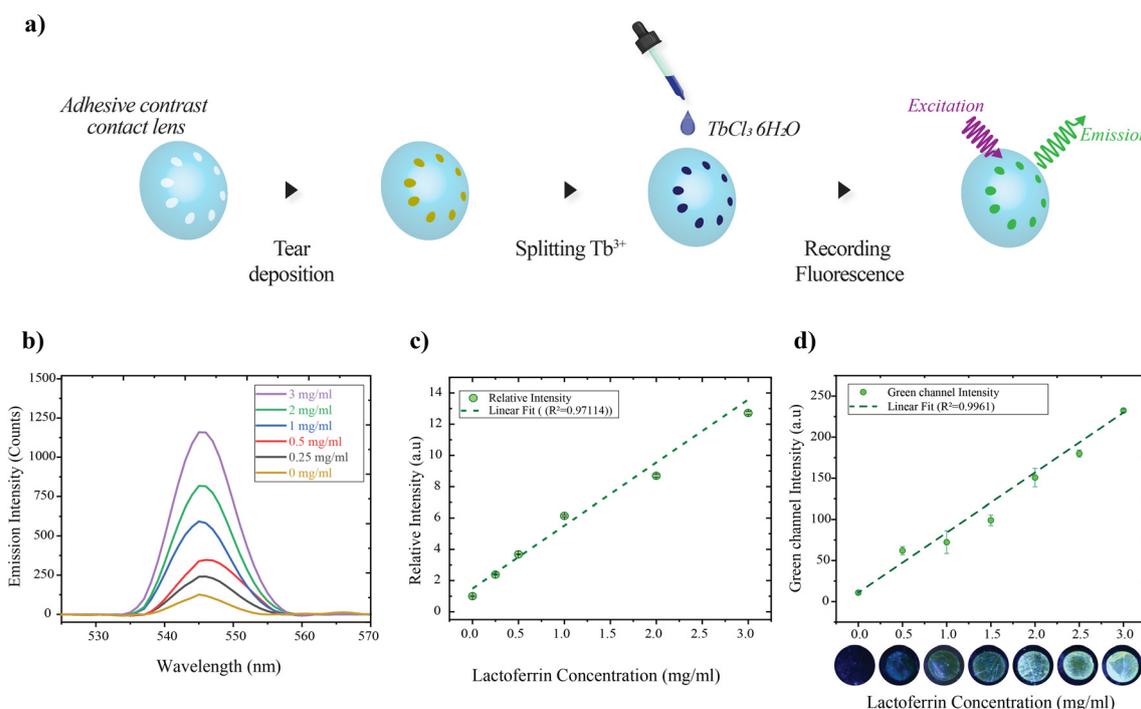

Fig. 5 a) Schematic of lactoferrin detection with fluorescence spectrometry; b) emission spectra of the lactoferrin–Tb complex on adhesive contrast surface; c) peak intensity change for 545 nm for various concentrations of lactoferrin; and d) colorimetric detection of lactoferrin with imaging the zones (2 mm diameter) under UV illumination and measuring the concentration-dependent green colour.

fluorophore (Tb^{3+}) is split on the surface of the lenses, which allows the complex formation and gives the green fluorescent emission on ultraviolet excitation. In the lab setting, droplets of lactoferrin with different concentrations in the physiological range are first split on the adhesive contrast surface, with zones of diameter 2 mm, followed by 1 mM of $TbCl_3 \cdot 6H_2O$ (in 50 mM Tris buffer, pH adjusted to 7.4 with hydrochloric acid). The fluorescence signal emitted from the sensing zones is captured under UV illumination (275 nm excitation). Fig. 5b presents the emission spectra of lactoferrin–Tb^{3+} for concentrations of 0 to 3 mg mL^{-1} for emission peaks at 545 nm. As the concentration of lactoferrin increases in the range, the emission intensity also increases with a variation in a near-linear fashion (Fig. 5c). This is because side chain tyrosine groups of lactoferrin have a high affinity for Tb^{3+}, and as lactoferrin concentrations rise, the complexation product increases, resulting in a stronger fluorescence signal. The lactoferrin level in the concentration range of 0.25 to 3 mg mL^{-1} is demonstrated.

Further, a more cost-effective colorimetric detection of lactoferrin is demonstrated. For this, lactoferrin of different concentrations was split across the adhesive contrast surface, followed by terbium ions (zone diameter 2 mm). The images were captured using a DSLR (Canon 1300D) under UV LED illumination (278 nm LED). The experimental setup schematic is shown in Fig. S8.† The intensity of the green channel of fluorescing zones was measured using ImageJ, and the average of three spots is plotted for different concentrations (Fig. 5d). The concentration-dependent colour change allows the measurement of lactoferrin in the range of 0.5 to 3 mg mL^{-1}. Tear fluid consists of various proteins and electrolytes, and the selectivity of the sensitizing interaction between Tb^{3+} and lactoferrin is crucial for the efficient probing of lactoferrin concentration (Table S1†). The interaction of different primary tear constituents with Tb^{3+} is studied by splitting different tear constituents on the adhesive contrast surface, followed by Tb^{3+} and recording the green channel signal. The selectivity study reveals that none of the primary tear constituents except lactoferrin resulted in a fluorescence signal (Fig. S9†).

Conclusions

An adhesive contrast contact lens for tear film splitting and analysis was fabricated, and its potential as a diagnostic platform was demonstrated. The adhesive contrast was fabricated on a PDMS-based contact lens *via* oxygen plasma-assisted selective grafting of silicone oil. The lubricant grafting transforms the high pinning into a non-adhesive surface by reducing the contact angle hysteresis by nearly 3.5 times. The substantial difference in the contact angle hysteresis between the pristine (41°) and oil-grafted PDMS (12°) facilitates adhesion difference-assisted droplet splitting. This novel approach allowed the tears to be collected in the predefined zones of the contact lens for further analysis *via* fluorescence spectroscopy as well as colorimetric studies. The

adhesive contrast contact lens integrated with a fluorescence spectrometer detected the lactoferrin level in the tears up to a concentration of 0.25 mg mL^{-1} when sensitized with terbium ions. Additionally, a cost-effective method of colorimetric detection of the fluorescence of the lactoferrin–terbium complex from the split tear fluid was demonstrated, and the concentration-dependent green color emission enabled the lactoferrin level detection in the physiological range up to 0.5 mg mL^{-1}. The developed contact lens platform is expected to be adaptable for sensing multiple biomolecules present in tears by integrating with a suitable probe in sensing areas.

Author contributions

Aravind M: methodology, investigation, data curation, and writing – original draft. Sajan D. George: conceptualization, supervision, project administration, funding acquisition, and writing – review & editing.

Conflicts of interest

There are no conflicts to declare.

Acknowledgements

References

1 N. M. Farandos, A. K. Yetisen, M. J. Monteiro, C. R. Lowe and S. H. Yun, *Adv. Healthcare Mater.*, 2015, **4**, 792–810.

2 Y. Shi, N. Jiang, P. Bikkannavar, M. F. Cordeiro and A. K. Yetisen, *Analyst*, 2021, **146**, 6416–6444.

3 Y. Zhu, S. Li, J. Li, N. Falcone, Q. Cui, S. Shah, M. C. Hartel, N. Yu, P. Young, N. R. de Barros, Z. Wu, R. Haghniaz, M. Ermis, C. Wang, H. Kang, J. Lee, S. Karamikamkar, S. Ahadian, V. Jucaud, M. R. Dokmeci, H.-J. Kim and A. Khademhosseini, *Adv. Mater.*, 2022, **34**, 2108389.

4 S. Kusama, K. Sato, S. Yoshida and M. Nishizawa, *Adv. Mater. Technol.*, 2020, **5**, 1900889.

5 M. Aravind, S. Chidangil and S. D. George, *Addit. Manuf.*, 2022, **55**, 102842.

6 Y. Zhu, R. Nasiri, E. Davoodi, S. Zhang, S. Saha, M. Linn, L. Jiang, R. Haghniaz, M. C. Hartel, V. Jucaud, M. R. Dokmeci, A. Herland, E. Toyserkani and A. Khademhosseini, *Small*, 2023, **19**, 2207017.

7 M. Elsherif, M. U. Hassan, A. K. Yetisen and H. Butt, *ACS Nano*, 2018, **12**, 5452–5462.

8 D. H. Keum, S. K. Kim, J. Koo, G. H. Lee, C. Jeon, J. W. Mok, B. H. Mun, K. J. Lee, E. Kamrani, C. K. Joo, S. Shin, J. Y. Sim, D. Myung, S. H. Yun, Z. Bao and S. K. Hahn, *Sci. Adv.*, 2020, **6**, eaba3252.

9 R. Moreddu, J. S. Wolffsohn, D. Vigolo and A. K. Yetisen, *Sens. Actuators, B*, 2020, **317**, 128183.

10 X. Deng, M. Korogiannaki, B. Rastegari, J. Zhang, M. Chen, Q. Fu, H. Sheardown, C. D. M. Filipe and T. Hoare, *ACS Appl. Mater. Interfaces*, 2016, **8**, 22064–22073.

11 Z. Zhu, L. Jin, F. Yu, F. Wang, Z. Weng, J. Liu, Z. Han and X. Wang, *Adv. Healthcare Mater.*, 2021, **10**, 2100259.

12 M. Willcox, N. Keir, V. Maseedupally, S. Masoudi, A. McDermott, R. Mobeen, C. Purslow, J. Santodomingo-Rubido, S. Tavazzi, F. Zeri and L. Jones, *Cont. Lens Anterior Eye*, 2021, **44**, 157–191.

13 M. Liu, S. Wang and L. Jiang, *Nat. Rev. Mater.*, 2017, **2**, 17036.

14 P. Vineeth, A. Peethan and S. D. George, *Chem. Eng. J.*, 2023, **459**, 141615.

15 A. M, A. Peethan and S. D. George, *Langmuir*, 2023, **39**, 1987–1996.

16 A. Peethan, M. Aravind, V. K. Unnikrishnan, S. Chidangil and S. D. George, *Appl. Surf. Sci.*, 2022, **571**, 151188.

17 J. E. George, V. K. Unnikrishnan, D. Mathur, S. Chidangil and S. D. George, *Sens. Actuators, B*, 2018, **272**, 485–493.

18 A. Peethan, A. M, S. Chidangil and S. D. George, *Lab Chip*, 2022, **22**, 4110–4117.

19 H. Torun, B. Fazla, S. Arman, B. Ozdalgic, A. Yetisen and S. Tasoglu, *Nano Sel.*, 2023, **4**, 79.

20 J. W. Jeong, M. M. P. Arnob, K.-M. Baek, S. Y. Lee, W.-C. Shih and Y. S. Jung, *Adv. Mater.*, 2016, **28**, 8695–8704.

21 M. H. M. Kouhani, J. Wu, A. Tavakoli, A. J. Weber and W. Li, *Lab Chip*, 2020, **20**, 332–342.

22 T. Y. Kim, J. W. Mok, S. H. Hong, S. H. Jeong, H. Choi, S. Shin, C.-K. Joo and S. K. Hahn, *Nat. Commun.*, 2022, **13**, 6801.

23 X. Ding, G. Ben-Shlomo and L. Que, *ACS Appl. Mater. Interfaces*, 2020, **12**, 45789–45795.

24 Z. Du, G. Zhao, A. Wang, W. Sun and S. Mi, *ACS Appl. Polym. Mater.*, 2022, **4**, 7290–7299.

25 R. Moreddu, V. Nasrollahi, P. Kassanos, S. Dimov, D. Vigolo and A. K. Yetisen, *Small*, 2021, **17**, 2102008.

26 K. A. Kwon, R. J. Shipley, M. Edirisinghe, D. G. Ezra, G. Rose, S. M. Best and R. E. Cameron, *J. R. Soc., Interface*, 2013, **10**, 20130227.

27 Y. Zhang, C. Lu and J. Zhang, *Nutrients*, 2021, **13**, 2492.

28 J. L. Flanagan and M. D. P. Willcox, *Biochimie*, 2009, **91**, 35–43.

29 H. An, G. Liu and V. S. J. Craig, *Adv. Colloid Interface Sci.*, 2015, **222**, 9–17.

30 Y. Shi, Y. Zhang, Y. Hu, R. Moreddu, Z. Fan, N. Jiang and A. K. Yetisen, *Sens. Actuators, B*, 2023, **378**, 133128.

31 P. Versura, P. Nanni, A. Bavelloni, W. L. Blalock, M. Piazzi, A. Roda and E. C. Campos, *Eye*, 2010, **24**, 1396–1402.

32 D. V. Seal, J. I. McGill, I. A. Mackie, G. M. Liakos, P. Jacobs and N. J. Goulding, *Br. J. Ophthalmol.*, 1986, **70**, 122.

33 R. J. Boukes, A. Boonstra, A. C. Breebaart, D. Reits, E. Glasius, L. Luyendyk and A. Kijlstra, *Doc. Ophthalmol.*, 1987, **67**, 105–113.

34 K. Yamada, S. Takaki, N. Komuro, K. Suzuki and D. Citterio, *Analyst*, 2014, **139**, 1637–1643.

35 K. Yamada, T. G. Henares, K. Suzuki and D. Citterio, *ACS Appl. Mater. Interfaces*, 2015, **7**, 24864–24875.